ALMA MATER STUDIORUM
UNIVERSITÀ DI BOLOGNA

ARCHIVIO ISTITUZIONALE
DELLA RICERCA

Alma Mater Studiorum Università di Bologna
Archivio istituzionale della ricerca

The Effects of Transient Overvoltages on the Reliability of HVDC Extruded Cables. Part 1: Long Temporary Overvoltages

This is the final peer-reviewed author's accepted manuscript (postprint) of the following publication:

Published Version:
Mazzanti G., Diban B. (2021). The Effects of Transient Overvoltages on the Reliability of HVDC Extruded Cables. Part 1: Long Temporary Overvoltages. IEEE TRANSACTIONS ON POWER DELIVERY, 36(6), 3784-3794 [10.1109/TPWRD.2021.3049269].

Availability:
This version is available at: https://hdl.handle.net/11585/814072 since: 2024-04-11

Published:
DOI: http://doi.org/10.1109/TPWRD.2021.3049269

Terms of use:

Some rights reserved. The terms and conditions for the reuse of this version of the manuscript are specified in the publishing policy. For all terms of use and more information see the publisher's website.

This item was downloaded from IRIS Università di Bologna (https://cris.unibo.it/).
When citing, please refer to the published version.

(Article begins on next page)

12 October 2024

The Effects of Transient Overvoltages on the Reliability of HVDC Extruded Cables. Part 1: Long Temporary Overvoltages

Giovanni Mazzanti, *Fellow, IEEE*, Bassel Diban, *Member, IEEE*

***Abstract*-- Extensive simulations have been carried out so far of transient voltages superimposed onto the DC voltage of HVDC cable transmission systems. With the advent of VSC HVDC cable systems, attention has turned to long Temporary Over-voltages in such systems. Preliminary experiments on the possible adverse effects of these long TOVs on the insulation of VSC HVDC cables have started, but no simulation models for estimating their effect on cable life and reliability have been developed yet. This investigation fills this gap by carrying out the simulative evaluation of the life lost by HVDC extruded cables subjected to long TOVs (Part 1) and switching impulses applied during Type Tests (Part 2), so as to compare the severity of these two transient voltages superimposed onto the DC voltage of HVDC extruded cables. This Part 1-paper is focused on estimating the severity of TOVs on extruded cable insulation by: calculating the electric field during the TOV; comparing it with the field during Type Test load cycles; using Miner's law of cumulated damage to calculate the life lost during the TOV, thereby also locating the most severely stressed point of insulation. In Part 2-paper, a similar evaluation for switching impulses and an overall comparison are performed.**

***Index Terms*-- Cross linked polyethylene insulation, HVDC insulation, Life estimation, Power cables, Reliability estimation, Switching transients, Surges.**

I. Introduction

Historically, broad simulations were performed of transient voltages superimposed onto the DC voltage of HVDC cable transmission systems. Especially external (for mixed cable-overhead lines) and internal overvoltages in Line-Commutated Current Source Converter (LCC) HVDC cables were investigated in [1], dating back to 1994. More recently, with the advent of Voltage Source Converter (VSC) HVDC cable systems, a big deal of simulations have been carried out to calculate overvoltages superimposed onto DC voltage in such systems [2]-[9]. To study the overvoltages experienced by VSC HVDC cable systems, the CIGRÉ Joint Working Group B4/B1/C4.73 has been formed, which is studying surge and extended over-voltage testing for HVDC cable systems [4] to identify and characterize temporary overvoltage shapes experienced by the cable within Modular Multilevel Converter (MMC) HVDC transmission systems in different configurations (monopolar, rigid bipolar). From these studies, a Technical Brochure is being prepared, which is supposed to include appropriate test levels and schemes [10].

G. Mazzanti and B. Diban are with the Dept. of Electrical, Electronic and Information Engineering "Guglielmo Marconi", University of Bologna, Viale Risorgimento 2, 40136 Bologna, Italy (e-mail: giovanni.mazzanti@unibo.it).

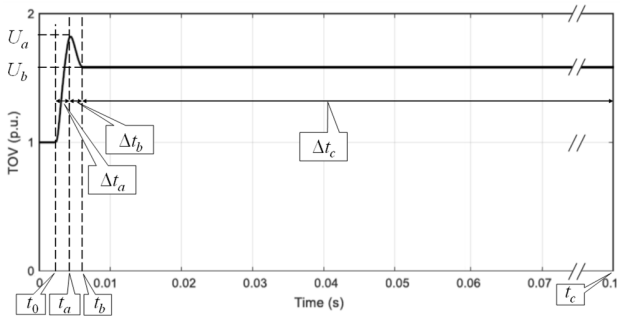

Fig. 1. Worst-case long TOV in VSC HVDC cable in symmetrical monopolar configuration (reprocessed from [3]).

TABLE I
ORDERS OF MAGNITUDE OF PARAMETERS OF WORST-CASE LONG TOV IN FIG. 1 (SYMMETRICAL MONOPOLAR CONFIGURATION)

parameter	name	value
U_a	peak voltage	≈1.8 (p.u. of rated voltage U_0)
U_b	plateau voltage	≈1.6 p.u. (p.u. of rated voltage U_0)
$\Delta t_a = t_a - t_0$	Time to Peak	≈5 ms
$\Delta t_b = t_b - t_a$	Time of peak decay	≈5 ms
$\Delta t_c = t_c - t_b$	Time of Plateau	≈100 ms

The simulations carried out in [2],[3], for the symmetric monopolar and in [4] for the rigid bipolar scheme highlight that especially in case of pole-to-ground faults in symmetric monopolar VSC HVDC cable systems, severe long Temporary Over-voltages (TOVs) may arise on the healthy pole - in rigid bipolar schemes, direct grounding limits overvoltage rise [3]. After fault, the healthy pole voltage would tend to 2 p.u. of the pre-fault DC voltage, but gets limited by the station surge arresters [3]. The level and duration of overvoltage depends on fault location, loading of line, surge arrester characteristics, DC cable length, grounding methods, etc. As one of the most severe situations, a pole-to-ground fault in the middle of the negative pole of a 225-km long low loaded symmetric monopolar VSC HVDC cable system was studied in [2], yielding a maximum overvoltage in the middle of the healthy positive pole up to 1.8 p.u. of the pre-fault DC voltage or even higher, with voltage rise time in the order of a few ms and overall duration around one hundred ms or more until cable is discharged [2,3].

This long TOV, referred to here as "worst-case TOV", is shown in Fig. 1; the indicative, but not exhaustive orders of magnitude of its parameters are listed in Table I to include

various possible cases. These values substantially encompass the waveforms obtained for similar cases in [5]-[10], but it should be highlighted that the waveshape in Fig. 1 holds for a symmetrical monopole; for rigid bipolar schemes the over-voltage peak and the plateau voltage are lower [3]-[9].

Let us point out again that this waveshape should be regarded as indicative, but not exhaustive of possible critical cases in VSC HVDC transmission systems. In fact, it should be agreed that the experience with HVDC VSC systems is not so well established as with HVDC LCC systems (this is also the main reason for the formation of CIGRÉ Joint Working Group B4/B1/C4.73). Therefore, it cannot be ruled out completely that other possible worst cases of levels and/or duration and/or waveshape of overvoltage might arise - in addition to the one presented here as "worst-case TOV" - from the analysis of other peculiar events in VSC HVDC systems, e.g. by changing cable line type, length and load, fault type and location, surge arrester features, grounding methods, etc. [10]. Anyway, whatever the waveform, a general methodology for a preliminary analysis of its effects on the extruded insulation of HVDC cables is really needed, as it is missing in existing documents on the subject.

Indeed, as to the authors' best knowledge, only a preliminary experimental evaluation of the possible adverse effects of this kind of long TOVs on the insulation of VSC HVDC cables has been started [11], while no simulation models aiming at estimating their effect on cable life and reliability have been developed so far. This investigation aims at filling this gap, by carrying out the simulative evaluation of the loss-of-life of HVDC extruded cables subjected to long TOVs (Part 1) and superimposed switching impulses (Part 2). In this way, the severity of long TOVs in terms of loss-of-life can be compared to that of switching impulses superimposed onto the DC voltage - applied during Type Tests for HVDC extruded cables after [12] - as the reference example of transient voltages.

This Part 1-paper focuses on a preliminary estimate of the severity of long TOVs in VSC HVDC systems on extruded cable insulation. Extruded cables are chosen, as polymeric DC cables are mainly associated with VSC type installations, where the cables are not subjected to polarity reversals in service [13]-[15]. Moreover, HVDC extruded cables are gaining market vs. mass impregnated non-draining (MIND) cables - with several HVDC extruded cable systems at 320-kV installed worldwide [14] and HVDC extruded cable systems commercially available at voltages up to ≈500-600 kV [16]-[18] - but their performance is not so well assessed as HVDC MIND cables.

The severity of long TOVs on HVDC extruded cables is estimated here by computing the total electric field during the TOV within cable insulation in both cold and hot conditions as the superposition of a DC steady-state field plus a transient AC field, and then comparing it with the field in Type Tests after CIGRÉ TB 496 [12] (as being a reference test stress for HVDC extruded cables). Thereafter Miner's law of cumulated damage is used together with the Inverse Power Model recommended by [12] to assess the effect of cumulated aging during the long TOV on the loss of life of the various points within cable insulation thickness. Eventually, this quantitative assessment of the effect of cable ageing during worst case TOV is compared against other degradation mechanisms that could be triggered at high fields, i.e. fast charge packets.

TABLE II

Values of τ_{inf} and $10\tau_{inf}$ after [12] vs. temperature θ in °C

θ [°C]	τ_{inf} [h]	τ_{inf} [s]	$10\tau_{inf}$ [h]	$10\tau_{inf}$ [s]
20	5.5	1.98×10^4	55	1.98×10^5
60	0.1	360	1	3600
70	0.042	151.2	0.42	1512
90	0.006	21.6	0.06	216

As a last, but not least remark, let us highlight that, although the methodologies employed in the work are themselves not new, drawing these methods together to demonstrate how they can be applied to assess the effect not only of long TOVs, but also of other transient voltage waveforms superimposed onto the DC voltage (see impulses in Part 2) is really important not only for researchers in the field, but also in particular to the cable industry. This is the first and foremost goal of this paper.

II. Field and Loss-of-Life Estimation for the Long TOV

A. Calculation of the Electric Field during the Long TOV

A preliminary assessment of the effect on extruded insulation of the worst-case long TOV for VSC HVDC cable systems (Fig.1 and Table I) requires the calculation of the electric field within cable insulation during such TOV. To attain this goal, the first thing to do is understanding which calculation method can be used in order to make the computation as simple and accurate at the same time as possible. In this respect, as suggested in [13], a clue comes from a comparison between the dielectric time constant $\tau=\varepsilon/\sigma$ (where ε and σ are, respectively, permittivity and electrical conductivity of the insulation) and the time intervals involved in the worst-case long TOV. The typical range of values of the dielectric time constant τ – as well as of time for stability 10 τ, i.e. the time to the attainment of the steady state distribution of electric field – for different materials typically used for DC extruded cables appear as a function of temperature θ [°C] in the Appendix A of [12]. The lower bounds of the ranges of τ, τ_{inf}, are listed vs. θ in Table II.

When comparing Tables I and II, it is readily seen that:

$$\Delta t_a = \Delta t_b \ll \Delta t_c \ll \tau \ll 10\,\tau \qquad (1)$$

Hence, although time intervals Δt_a, Δt_b, Δt_c are fairly different from each other ($\Delta t_a \approx \Delta t_b \ll \Delta t_c$), they are all much lower than the typical lower bounds of time constant τ "*for different materials that are likely to be used for DC extruded cables*" [12]. This holds not only for the minimum value of τ in Table II (i.e. that at 90°C), but also a fortiori for the maximum value at 20°C (room temperature), as well as for whatever lower temperature, either in the lab or in service.

Therefore, both when the cable is hot, i.e. fully loaded (mostly with service temperature θ_S=70°C, a few times with θ_S=90°C [14],[18]) and a fortiori when the cable is cold (≈room temperature, 20°C), the characteristic time intervals Δt_a, Δt_b, Δt_c of the long TOV of Fig. 1 are much shorter than the time constant and (a fortiori) than the time for stability 10τ of typical

polymeric extruded insulation for HVDC cables. As a consequence, the worst-case TOV should not perturb the pre-existing resistive electric field due to rated DC voltage U_0; such resistive field can be assumed to have already reached steady state for the purpose of evaluating the total electric field during the worst-case TOV. Hence, let us follow the guidelines found in the milestone paper [19] about DC field computation in homogeneous dielectrics, and calculate the total electric field $E_{TOV}(r,t)$ at each single radial coordinate r within HVDC cable insulation thickness and at each single time t within intervals Δt_a, Δt_b, Δt_c as the superposition of

- $E_{DC,U0}(r)$, the resistive steady-state DC field due to U_0, referred to as DC field here, consistently with [14],[19];
- $E_{AC}(r,t)$, the capacitive field controlled by dielectric permittivity associated with the long TOV $U(t)$ as it exceeds U_0 during time intervals Δt_a, Δt_b, Δt_c, referred to for brevity as AC[1] field here, consistently with [14],[19]:

$$E_{TOV}(r,t)=E_{DC,U0}(r)+E_{AC}(r,t) \qquad (2)$$

This method makes the TOV field calculation simple and effective, as aimed at above, and can be applied also to impulse voltages superimposed onto a DC voltage, see Part 2-paper.

Under the above assumption that the HVDC cable insulation is homogeneous, the resistive steady-state DC field $E_{DC,U0}(r)$ can be calculated via the following expression that includes the effect of temperature and field dependence [14],[19]:

$$E_{DC,U0}(r) = U_0 \frac{r^{z-1}\, exp\{-b[E_{DC,U0}(r)]\}}{\int_{r_i}^{r_o} r'^{z-1}\, exp\{-b[E_{DC,U0}(r')]\}\, dr'} \qquad (3)$$

$$z = a\Delta T / \ln(r_o/r_i) \qquad (4)$$

$$\Delta T(r) = T(r) - T(r_o) = [W_C/(2\pi\lambda_{T,d})]\, \ln(r_o/r) \qquad (5)$$

where:

- r_i = inner radius of cable insulation;
- r_o = outer radius of cable insulation;
- $r \in [r_i, r_o]$ = radial coordinate within cable insulation;
- ΔT = temperature drop across insulation thickness;
- W_C = conductor losses per unit of length;
- $\lambda_{T,d}$ = thermal conductivity of insulation;
- a = temperature coefficient of electrical conductivity;
- b = electric field coefficient of electrical conductivity.

Equation (3) is consistent with the following empirical relationship often used to describe the dependence of the volume electrical conductivity σ of solid dielectrics on DC electric field E and absolute temperature T (see, e.g. [14],[20]):

$$\sigma(T,E) = \sigma_0\, exp[\, a(T - T_0) + b(E - E_0)] \qquad (6)$$

where σ_0 represents insulation electrical conductivity at reference temperature T_0 and electric stress E_0.

Relationship (3) is a transcendent equation, since the unknown $E_{DC,U0}(r)$ appears at both left- and right-hand side, and can be solved only numerically. Thus, it is replaced here with the well-known Eoll's formula [21] (used since 1975 for practical and preliminary evaluation purposes), a closed form relationship for steady state DC field obtained by Eoll from (3) via simplifying hypotheses holding fairly well apart from very thick insulation and strongly non-uniform DC field - which is not the case of the cable treated in Section III. Eoll's formula is as follows [14],[21]:

$$E_{DC,U0}(r) = \delta U_0 (r/r_o)^{\delta-1} / \{r_o[1 - (r/r_o)^{\delta}]\} \qquad (7)$$

$$\delta = \left[\frac{a\Delta T}{ln(r_o/r_i)} + \frac{bU_{DC}}{(r_o - r_i)}\right] / \left[1 + \frac{bU_{DC}}{(r_o - r_i)}\right] \qquad (8)$$

where δ is the so-called "field inversion coefficient". Indeed, δ rises with cable current and if δ>1 the "electric field inversion" in the insulation wall of HVDC cables occurs as the load rises from 0 to full: the highest electric field is found at the inner insulation when δ<1 and at the outer insulation when δ>1 [14].

The capacitive component of the electric field, $E_{AC}(r)$, can be expressed according to the well-known following formula, whereby the field/potential distribution is ruled by dielectric permittivity ε [14],[19]:

$$E_{AC}(r,t) = [U(t) - U_0]/[r\, ln(r_o/r_i)] \qquad (9)$$

After these considerations, a preliminary evaluation of the severity of the electric field during the worst-case TOV for an HVDC extruded cable is carried out here in the following steps.

1) Choice of a typical case-study HVDC extruded cable.
2) Calculation for this cable in
   i) Cold Cable conditions, i.e. zero load current;
   ii) Hot Cable conditions, i.e. full load current;
   of the following quantities:
   a) temperature profiles $T(r)$. In steady-state, temperature is computed at each radial coordinate r within cable insulation according to Standard IEC 60287 [22], while during thermal transients - e.g. in Load Cycle Type Tests after [12] - temperature is computed at each r and at each time t of the thermal transient using the CIGRÉ transient thermal network model of the cable, as recommended in Standard IEC 60853 [23];
   b) DC field $E_{DC,U0}(r)$ at voltage $U_{DC}=U_0$ through (7);
   c) DC conductivity σ through (6) and time constant τ=ε/σ for the Cold Cable and the Hot Cable;
   d) capacitive AC field $E_{AC}(r)$ at voltage $U(t)$ - U_0 during the TOV through (9);
   e) total field $E_{TOV}(r,t)$ through (2);
   f) DC field $E_{DC,UT}(r)$ at voltage U_T = 1.85 U_0 in Load Cycle Type Tests (LCTT) after [12], which is a quite challenging and reference test in the qualification procedure of HVDC extruded cables.
3) Comparison of $E_{TOV}(r,t)$ with $E_{DC,UT}(r)$ to assess the severity of TOV field vs. the reference LCTT field.

Calculations at above points 2b), 2c), 2f) - relevant to the DC

[1] Transient voltages/fields varying much faster than the dielectric time constant τ=ε/σ are ruled by the dielectric permittivity ε of the insulation and should be treated with the methods developed for capacitive AC fields, even if the voltage/field does not actually change polarity [14],[19].

field component, see next Figs. 3, 4 - rely on three different sets of conductivity coefficients a, b of the insulation:

I) the "low set", a_L=0.042 K^{-1}, b_L=0.032 mm/kV;
II) the medium set, a_M=0.084 K^{-1},b_M=0.0645 mm/kV;
III) the "high set", a_H=0.101 K^{-1}, b_H=0.0775 mm/kV.

The low set a_L,b_L, the medium set a_M,b_M and the high set a_H,b_H fall, respectively, at the lower bound, in the middle and at the upper bound of the typical range of variation of onductivity coefficients for DC-XLPE compounds [20],[24]-[26], so as to perform a sensitivity analysis of the field during the TOV to different types of cross-linked compounds likely to be used for HVDC extruded cable insulation.

B. Estimation of the Life Fraction Lost during the TOV

A more quantitative assessment of the severity of the worst-case TOV of Fig. 1 for the extruded insulation for HVDC cables can be achieved by evaluating the aging effects cumulated during the TOV in terms of life lost at the various points within cable insulation thickness. This can be done resorting to Miner's law of cumulated damage/aging [27], applied for the life estimation of HVAC cables [28],[29] and later on also of HVDC cables [24],[25] in the presence of time-varying electro-thermal stress. In summary, Miner's law is based on the observation that in HV cables subjected to time-varying electro-thermal stress - e.g. due to load cycles as in [24],[25],[28],[29], or due to the time variation of applied voltage as in the presence of the long TOV, or of switching impulses as in Part 2 of this study - the cable can be assumed to fail as its insulation fails because of the electro-thermal aging cumulated at the most severely stressed point $r^*\in[r_i,r_o]$ within cable insulation. This aging can be estimated by evaluating the "infinitesimal loss-of-life fraction" $dLF(r^*,t)$ relevant to each infinitesimal interval dt between t and $t+dt$ wherein electro-thermal stress (temperature $T(r^*,t)$ and electric field $E(r^*,t)$) can be deemed as constant:

$$dLF(r*,t) = dt/L[E(r*,t),T(r*,t)] \qquad (10)$$

where $L[E(r^*,t),T(r^*,t)]$ is life at electric field $E(r^*,t)$ and temperature $T(r^*,t)$. This life can be estimated resorting to a proper life model for cable insulation subjected to constant values of temperature $T(r^*,t)$ and electric field $E(r^*,t)$.

Therefore, the "total loss-of-life fraction" $\Delta LF(r^*)$ relevant to the total time period Δt_P where stress varies according to a known time pattern - e.g. a daily load cycle of cable current, as in [24],[25],[28],[29], or the worst-case TOV of Fig. 1 – can be determined by integrating over Δt_P the infinitesimal loss-of-life fractions $dLF(r^*,t)$, as follows:

$$\Delta LF(r^*) = \int_{\Delta t_P} dLF(r^*) = \int_{\Delta t_P} \frac{dt_P}{L[E(r^*,t_P),T(r^*,t_P)]} \qquad (11)$$

Now, the severity of the TOV for the HVDC extruded cable insulation can be quantified by calculating the total loss-of-life fraction $\Delta LF_{TOV}(r^*)$ via (11), where $L=f[E(r^*,t_P),T(r^*,t_P)]$ is a proper life model for cable insulation subjected to constant values – at a given time $t_P\in\Delta t_P=\Delta t_a+\Delta t_b+\Delta t_c$ during the TOV – of electric field $E(r^*,t_P)$ and temperature $T(r^*,t_P)$. This model is required to compute the total loss-of-life fraction $\Delta LF_{TOV}(r^*)$ through (11) from the values of electric field $E(r^*,t_P)$ and temperature $T(r^*,t_P)$ vs. time $t_P\in\Delta t_P$ during the TOV.

In fact, during the worst-case TOV - lasting ≈100 ms, much less than the thermal time constant of HV cables [30] - cable temperature at the most severely stressed point r^* can be assumed as constant, i.e. $T(r^*,t_P)=T_P(r^*)$=const, and equal to either the Cold or the Hot Cable temperature. Then, the required insulation life model can be focused on the dependence of cable life on electric field $E(r^*,t_P)=E_P(r^*)$, $t_P\in\Delta t_P$, i.e on function $L=f[E_P(r^*)]$. To find this function, the so-called Inverse Power Model (IPM) after [12] can be taken for expressing the relationship between voltage and time-to-failure, i.e. [12],[14]:

$$U^n L = \text{constant} \qquad (12)$$

where:
U = applied voltage;
L = time to failure (life) at constant applied voltage U;
n=life exponent or Voltage Endurance Coefficient (VEC).

To eliminate the arbitrary constant in (12), an equivalence can be set between the factor $U^n L$ at a generic voltage U and at rated voltage U_0. Then $U^n L = U_0^n L_0$, where L_0 is design life of the cable, and (12) can be rewritten as follows:

$$L = L_0 (U_0/U)^n \qquad (13)$$

It is worth emphasizing here that, due to the random (stochastic) behavior of the insulation, the probabilistic approach to HV cable design is usually followed [31]. This involves that cable life L is meant as the time to the attainment of a given failure probability, P, or – equivalently – of a certain reliability R=1-P. Typically, the life L of HV extruded cables follows the Weibull probability distribution function (pdf), thus the relationship between L and R is as follows [32]:

$$R(L)=1-P(L)=\exp[-(L/\alpha_t)^{\beta_t}] \qquad (14)$$

where α_t is the scale parameter of the Weibull pdf and depends on applied stresses; β_t is the shape parameter of the pdf. Relationship (14) implies that the lower the life L, the lower the reliability after a service time equal to L, and vice versa; more generally, a fraction of life lost - see Table VIII - at a given failure probability implies a reduction of cable reliability.

As shown in [14], relationship (13) can be extended to electric field (stress) during the TOV at the most stressed point within cable insulation, $E_P(r^*)$, thereby attaining function $L=f[E_P(r^*)]$:

$$L = L_0 [E_0/E_P(r^*)]^n \qquad (15)$$

where E_0 is the design field at the most stressed point within cable insulation. In other words, cable insulation is designed and manufactured so that its most stressed point can withstand an electric field E_0 for a service time $\geq L_0$ in the reference design conditions of the cable. Such conditions are usually the above-defined Hot Cable conditions, giving rise to the most severe electro-thermal stress for cable insulation either at inner or outer insulation, depending on the values of conductivity coefficients a, b: when a field inversion occurs (δ>1, see (8)), the most

severe electro-thermal stress is expected at outer insulation, while if no field inversion occurs (δ<1), the most severe electro-thermal stress is expected at inner insulation [14].

Relationship (15) with L_0=40 years and n=10 is used here to express $L[E(r^*,t_P),T(r^*,t_P)]$ in (11) so as to calculate the total loss-of-life fraction $\Delta LF_{TOV}(r^*)$ during TOVs. In (15), values of L_0=40 years and of n=10 are taken, first and foremost since they are recommended in [12], the most authoritative reference for design and testing of HVDC extruded cable systems so far. Moreover, once design life L_0 is fixed to 40 years, the n=10 hypothesis leads to the test voltage U_T=1.85U_0 prescribed for the 30 days overall duration of load cycle type tests (LCTT) according to [12]. Since TOV fields are compared here with LCTT fields at U_T=1.85U_0, we want to make such comparison fully consistent with the prescriptions after [12], and loss-of-life estimation consistent with such comparison. As mentioned in [12], n=10 is a lower limit value: indeed, values of n in excess of 10 have been obtained for newly-developed and better performing extruded insulation for HVDC cables [14], thus the value n=10 is more conservative, so as to encompass also less performing extruded compounds.

Let us emphasize that (15) can be used in the presence of both the DC and the AC component of TOV field (2), since – as shown in [33] - the IPM model with L_0=40 years and n=7 is used for EHV-AC extruded cables in Standard IEC 62067 to establish prequalification test duration and voltage level. Of course, n=10 is preferred here as we deal with HV-DC cables.

III. Case Study

A. Case-Study Cable

In this applicative section, let us focus for brevity on one single case-study cable type (similar results are obtained for other cable types, differing as for rated voltage, ampacity, etc.). It is a land XLPE-insulated HVDC cable for use with VSC, with typical maximum voltage and power ratings of 320 kV and ≈1,000 MW, respectively. In particular, the reason for choosing 320 kV as the rated voltage is because a noteworthy overall length of such rated voltage cables – for both land and sea usage - has already been commissioned [34],[35], while only one higher-voltage-rated cable is presently in service [18]. The main design parameters are copper conductor cross section S=1,600 mm^2, DC-XLPE insulation thickness s≈18 mm, rated current (ampacity) I_D=1,727 A, rated conductor temperature θ_D=70°C. Other design parameters are listed in Table III [24],[25].

B. Temperature Profiles for the Hot and Cold Cable Condition

For the case-study cable, the transient temperature profiles during one 24-hour load cycle for prequalification tests (PQT) and type tests (TT) according to [12] are reported in Fig. 2 [25]. In such 24-hour load cycles, the conductor temperature is: 1) increased via current heating from room temperature θ_a to a temperature ≥ rated conductor temperature θ_D in the first 6 h (1st step); 2) maintained at or above θ_D during the next 2 h (2nd step) by keeping the rated current throughout the step; 3) reduced to θ_a via natural cooling over the next 16 h (3rd step); 1st and 2nd steps are called "heating" period, 3rd step "cooling" period.

TABLE III
Case-study Cable Characteristics

Parameter	Value
Rated power (bipolar scheme) [MW]	1,105
Rated voltage [kV]	320
Conductor Material	Cu
Insulation Material	DC-XLPE
relative permittivity ε_r	2.3
Rated conductor temperature θ_D [°C]	70
Ambient temperature θ_a [°C]	20
Conductor cross-section [mm^2]	1600
inner insulation radius r_i [mm]	24.6
Insulation thickness [mm]	17.9
outer insulation radius r_o [mm]	42.5
Design life L_D [years]	40
Design failure probability P_D [%]	1
Rated current [A]	1,727

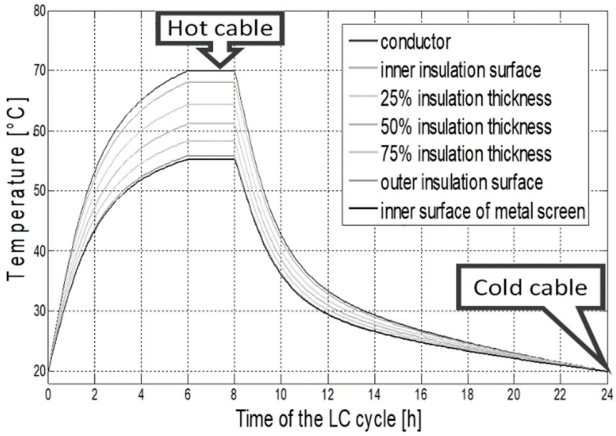

Fig. 2. Transient temperatures during one 24-h load cycle. After [25].

The steady-state temperature reached within the insulation during the 2nd step can be taken as the Hot Cable temperature profile, while the room temperature θ_a can be taken as the Cold Cable uniform temperature profile within the insulation.

C. DC Field during Load Cycle Type Test (LCTT)

The DC steady-state field profiles at rated voltage U_0=320 kV within the insulation of the case-study cable computed via (7) with the low set a_L,b_L of temperature and field coefficients of conductivity for the Cold and Hot Cable temperature profiles in Fig. 2 are plotted in Fig. 3; DC LCTT electric field profiles at U_T=1.85U_0=592 kV for the Cold and Hot Cable are also displayed. Figure 3 shows that with a_L,b_L a field inversion does not take place as the case-study cable passes from zero to full load, not only at U_0, but also at U_T=1.85U_0. Thus, the maximum field stays at the inner insulation as the load current goes from 0 to cable ampacity, although minimum and maximum field become very close to each other. The main features of DC field – i.e. minimum and maximum values at inner and outer insulation with voltage U_0 and U_T – obtained for the cold and hot case-study cable with a_L,b_L are summarized in Table IV.

From the field profiles in Fig. 3, the corresponding profiles of conductivity and time constant $\tau=\varepsilon/\sigma$ within the insulation wall with the low set a_L,b_L for the Cold and Hot Cable have been calculated: they are omitted here for brevity. In summary, for the Cold Cable in LCTT conditions τ ranges from 6.8 h at inner insulation to 9.9 h at outer insulation, while for the Hot Cable

in LCTT conditions τ ranges from 1.1 h at inner insulation to 1.9 h at outer insulation. It can be concluded that with the low set a_L,b_L for both the Cold and the Hot Cable the variation of τ within cable insulation is not so dramatic as to involve strongly different charge dynamics processes within the insulation itself during the LCTT. The same holds also at rated voltage U_0. Of course, this is valid for a uniform cable insulation as that implicitly considered here, which is not affected by local inhomogeneities and local distributions of space charge both at electrodes and in the insulation bulk.

The DC steady-state field profiles at U_0 within the insulation of the case-study cable computed via (7) with the high set a_H, b_H of temperature and field coefficients of conductivity for the Cold and the Hot Cable temperature profiles in Fig. 2 are plotted in Fig. 4; LCTT field profiles at U_T=1.85U_0 for the Cold and the Hot Cable are also displayed. Figure 4 shows that with a_H,b_H a field inversion takes place as the case-study cable passes from zero to full load, not only at U_0, but also at U_T=1.85U_0, so that the maximum field moves from inner to outer insulation as the load current goes from 0 to cable ampacity. The inversion, also occurring with the medium set a_M,b_M – omitted here for brevity – is much sharper with a_H, b_H. The main features of DC field – i.e. minimum and maximum values at inner and outer insulation with voltage U_0 and U_T – obtained for the cold and hot case-study cable with a_H,b_H are summarized in Table V.

From the field profiles in Fig. 4, the corresponding profiles of conductivity and time constant τ=ε/σ within the insulation wall with the high set a_H,b_H for the Cold and Hot Cable have been calculated: they are omitted here for brevity. In summary, for the Cold Cable in LCTT conditions τ ranges from 0.4 h at inner insulation to 0.8 h at outer insulation, while for the Hot Cable in LCTT conditions τ ranges from 6.6×10^{-3} h at inner insulation to 0.011 h at outer insulation. Again, it can be concluded that also with the high set a_H,b_H - like with the low set a_L,b_L - for both the Cold and the Hot cable the variation of τ within cable insulation does not involve strongly different charge dynamics processes within the insulation.

It should be pointed out that:

1) for the Cold Cable the field profiles in Figs. 3,4 can be conservatively taken as equal to those at the end of the cooling period of 24-h and especially 48-h loading cycles after [12]. Indeed, at that time the attainment of steady-state electric field is not granted - due to the high value of dielectric time constant at room temperature, see Table II – but the Cold Cable profiles in Figs. 3, 4 yield the maximum possible values of electric field at inner insulation in LCTT, thus they are conservative;

2) for the Hot Cable the field profiles in Figs. 3,4 can be conservatively taken as equal to those at the end of the 2-h heating period of 24-h and 48-h TT loading cycles after [12]. Indeed, at that time the attainment of steady-state electric field is practically granted, since at θ_D=70÷90°C the time for stability 10τ is < 2 h for typical DC extruded insulation (see Table II).

D. Field during the TOV

Figures 5, 6 and 7 show the AC electric field $E_{AC}(r,t)$ vs. time respectively during time intervals Δt_a, Δt_b, Δt_c of the TOV at 5 locations within the insulation of the case-study cable computed

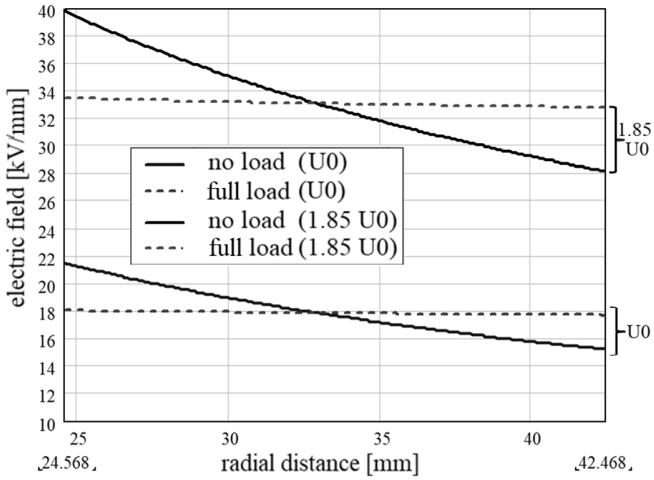

Fig. 3. Electric field profiles within the insulation of case-study cable at rated voltage U_0 with the low set a_L,b_L for the Cold and the Hot Cable. Type-test electric field profiles at U_T=1.85U_0 are also shown.

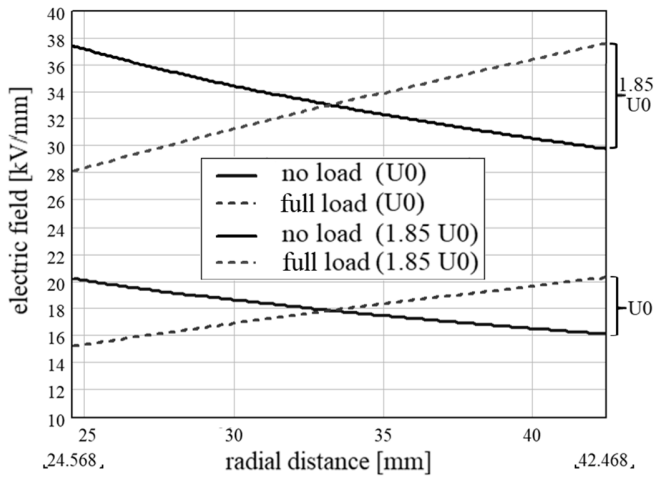

Fig. 4. Same as 3, but with the high set a_H,b_H.

TABLE IV
DC FIELD FEATURES OF CASE-STUDY CABLE OBTAINED WITH a_L,b_L

	Cold Cable		Hot Cable	
Voltage ↓	field at inner insulation	field at outer insulation	field at inner insulation	field at outer insulation
U_0=320 kV (design)	E_{max}=21.5 kV/mm	E_{min}=15.2 kV/mm	E_{min}=18.1 kV/mm	E_{max}=17.7 kV/mm
U_T=592 kV (LCTT)	E_{max}=39.8 kV/mm	E_{min}=28.1 kV/mm	E_{min}=33.4 kV/mm	E_{max}=32.8 kV/mm

TABLE V
DC FIELD FEATURES OF CASE-STUDY CABLE OBTAINED WITH a_H,b_H

	Cold Cable		Hot Cable	
Voltage ↓	field at inner insulation	field at outer insulation	field at inner insulation	field at outer insulation
U_0=320 kV (design)	E_{max}=20.2 kV/mm	E_{min}=16.1 kV/mm	E_{min}=15.2 kV/mm	E_{max}=20.3 kV/mm
U_T=592 kV (LCTT)	E_{max}=37.4 kV/mm	E_{min}=29.7 kV/mm	E_{min}=28.1 kV/mm	E_{max}=37.6 kV/mm

by means of (9) with $U(t)$ according to the TOV of Fig. 1. It is worth pointing out that this TOV has such a waveshape that the transient voltage component $U(t)$-U_0 can be easily modeled as three piecewise-linear components in sequence. In practice, the linear parts of these piecewise components are smoothly linked to one another, as readily seen by zooming-in Fig. 1, but – for

the sake of simplicity – they are regarded here as a sequence of:

- a pure linear-increasing waveshape over time Δt_a;
- a pure linear-decreasing waveshape over time Δt_b;
- a constant (plateau) waveshape over time Δt_c.

This gives rise to the "angular points" found by flanking Figs. 5, 6 and 7 one after another (see also next Figs. 8-11). A more careful representation of the TOV including smoother non-linear links between one linear piece and the subsequent is of course possible, but it would change neither the method of field calculation (based on (2),(7)-(9)) nor the results obtained.

At this stage, total field can be calculated. For the low set a_L,b_L Figure 8 displays the total electric field in the insulation wall of the Cold Cable vs. time during the whole TOV at 5 locations within the insulation of the chosen cable, calculated through (2) as the superposition of DC field at U_0 for the Cold Cable plotted in Fig. 3 plus the AC field during the whole TOV – i.e. the sequence of Δt_a, Δt_b, Δt_c – illustrated in Figs. 5, 6, 7; Figure 9 is the same as Fig. 8, but for the Hot Cable.

Similarly, for the high set a_H,b_H Figure 10 reports the total electric field in the insulation wall of the Cold Cable vs. time during the whole TOV at 5 locations within the insulation of the chosen cable, calculated through (2) as the superposition of DC field at U_0 for the Cold Cable plotted in Fig. 4 plus the AC field during the whole TOV shown in Figs. 5, 6, 7; Figure 11 is the same as Fig. 10, but for the Hot Cable.

Figures 8-11 emphasize that the maximum field during the TOV is always at inner insulation due to the AC field, which is always maximum at inner insulation, see (9). Thus, inner insulation is always the most stressed point during the TOV.

E. Field during the TOV vs. DC Field during LCTT

In Table VI a comprehensive comparison relevant to the low set of conductivity coefficients a_L,b_L is reported, i.e. the highest total field due to the TOV within Δt_a, Δt_b, Δt_c at inner and outer insulation for the Hot and Cold Cable (see Figs. 8, 9) vs. the highest DC field during the LCTT at inner and outer insulation (see Fig. 3). Similarly, in Table VII a comprehensive comparison relevant to the high set of conductivity coefficients a_H,b_H is reported, i.e. the highest total field due to the TOV within Δt_a, Δt_b, Δt_c at inner and outer insulation for the Hot and Cold Cable (see Figs. 10, 11) vs. the highest DC field during the LCTT at inner and outer insulation (see Fig. 4). Cases when the TOV field exceeds the LCTT field are highlighted in light grey for the Cold Cable, in dark grey for the Hot Cable, since these cases are, strictly speaking, not encompassed by the LCTT as for the field level applied during this test.

Table VI shows that with the low set a_L,b_L:

- for the Cold Cable the maximum field during the TOV at inner insulation (40.6 kV/mm for t=t_a) is higher than the maximum field at inner insulation during the cold part (=end) of the 24-h and 48-h LCTT (39.8 kV/mm);
- for the Hot Cable the maximum field during the TOV at inner insulation (37.1 kV/mm for t=t_a) is higher than the maximum field at inner insulation during the hot part of the 24-h and 48-h LCTT (33.4 kV/mm).

Table VII shows that with the high set a_H, b_H:

- for the Cold Cable, the maximum field during the TOV at inner insulation (39.3 kV/mm for t=t_a) is higher than the maximum field at inner insulation during the cold part of the 24-h and 48-h LCTT (37.4 kV/mm);
- for the Hot Cable, the maximum field during the TOV at inner insulation (34.2 kV/mm for t=t_a) is higher than the maximum field at inner insulation during the hot part of the 24-h and 48-h LCTT (28.1 kV/mm).

Tables VI, VII also show that the situation for the Hot cable is worse than for the Cold cable, especially with a_H,b_H. Indeed:

- the maximum field at inner insulation during the TOV exceeds that during the LCTT more widely for the Hot than for the Cold Cable;
- for the Cold Cable at inner insulation the field during the TOV exceeds the field during the LCTT for a quite short

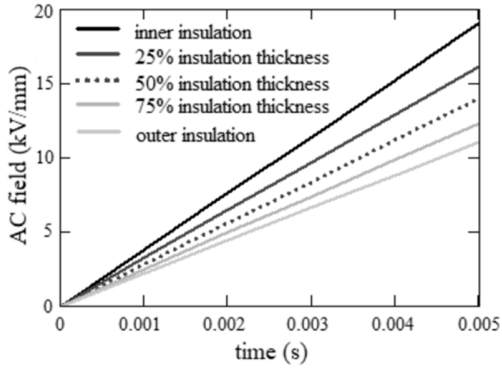

Fig. 5. AC electric field during time interval Δt_a of the TOV vs. time at 5 locations within the insulation of the case-study cable

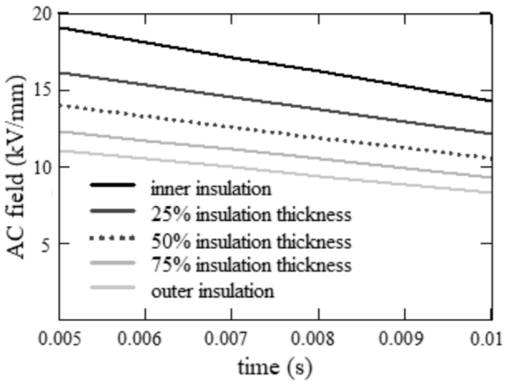

Fig. 6. AC electric field during time interval Δt_b of the TOV vs. time at 5 locations within the insulation of the case-study cable

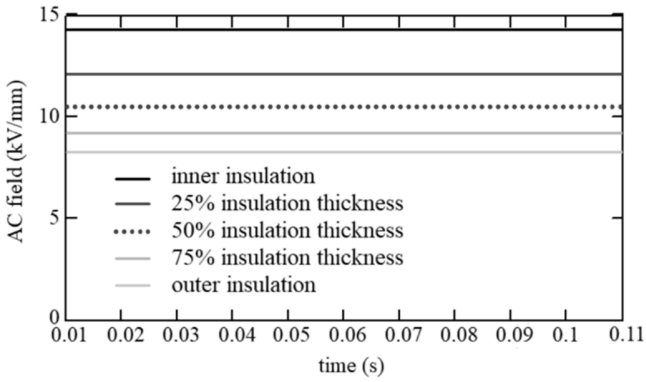

Fig. 7. AC electric field during time interval Δt_c of the TOV vs. time at 5 locations within the insulation of the case-study cable

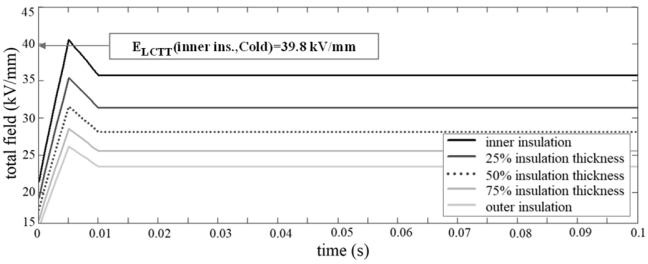

Fig. 8. Total electric field for the Cold Cable vs. time during the whole TOV at 5 locations within the insulation of the chosen cable with the low set a_L,b_L

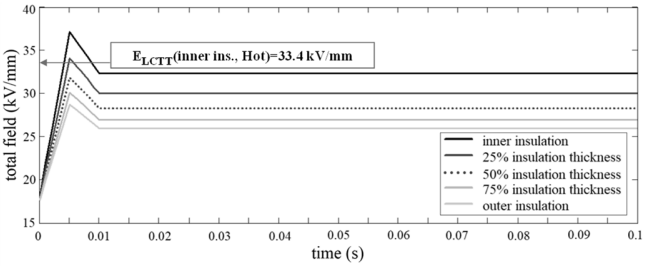

Fig. 9. Total electric field for the Hot Cable vs. time during the whole TOV at 5 locations within the insulation of the chosen cable with the low set a_L,b_L

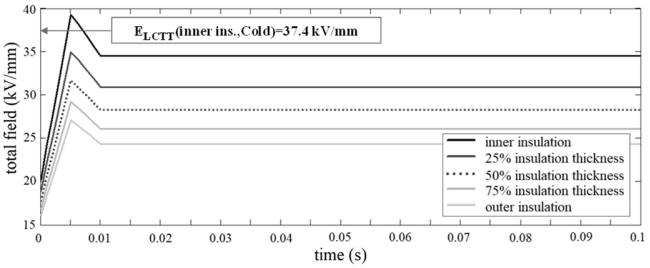

Fig. 10. Total electric field for the Cold Cable vs. time during the whole TOV at 5 locations within the insulation of the chosen cable with the high set a_H,b_H

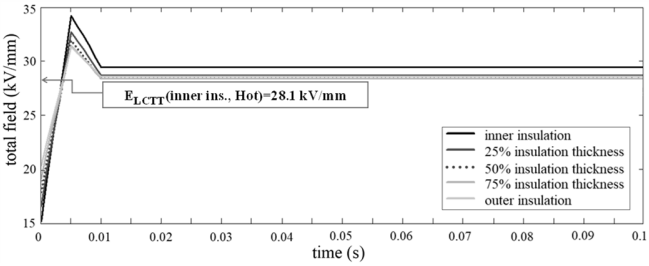

Fig. 11. Total electric field for the Hot Cable vs. time during the whole TOV at 5 locations within the insulation of the chosen cable with the high set a_H,b_H

time, i.e. ≈1 ms around t_a at most (see Fig. 1). For the Hot Cable, this holds with a_L,b_L, but with a_H,b_H it can be seen that throughout Δt_c the maximum TOV field at inner insulation (29.5 kV/mm) exceeds the field during the LCTT (28.1 kV/mm), thus for a much longer time, ≈0.1 s.

This is because the DC field at inner insulation is minimum for the Hot Cable, maximum for the Cold Cable, while the AC field component of the TOV is maximum at inner insulation. The worsening of the situation during the TOV for the Hot Cable at inner insulation as the values of a,b increase is due to the progressive field inversion associated with such increase and is confirmed by many simulations – omitted for brevity – done with other sets of a,b in-between a_L,b_L and a_H,b_H.

F. Results of Loss-of-Life Fraction Calculation during the TOV

Table VIII lists the values of total loss-of-life fractions at inner insulation – the most stressed point – calculated according to (11) for the TOV of Fig. 1 with a_L,b_L, a_M, b_M and a_H,b_H, thus based on $E(r^*=r_i,t_P)$ with $t_P \in \Delta t_P=\Delta t_a+\Delta t_b+\Delta t_c$ from Figs. 8,10 for the Cold Cable, Figs. 9,11 for the Hot Cable. Since $\Delta t_c \approx 100$ ms in Table I is an order-of-magnitude value, life lost has also been calculated for Δt_c=200 ms as a possible upper limit of Δt_c guessed from the various simulations done so far [2]-[10].

TABLE VI
HIGHEST TOTAL FIELD DUE TO THE TOV OF FIG. 1 WITHIN Δt_a, Δt_b, Δt_c VS. HIGHEST DC FIELD AT LCTT VOLTAGE, WITH a_L,b_L

Voltage	Hot/Cold cable	Time interval	Duration (ms)	Max.field at inner insul.(kV/mm)	Max.field at outer insul.(kV/mm)
TOV	Cold	Δt_a	≈5	40.6 (at t_a)	26.2 (at t_a)
TOV	Cold	Δt_b	≈5	40.6 (at t_a)	26.2 (at t_a)
TOV	Cold	Δt_c	≈100	35.8(constant)	23.4(constant)
TOV	Hot	Δt_a	≈5	37.1 (at t_a)	28.7 (at t_a)
TOV	Hot	Δt_b	≈5	37.1 (at t_a)	28.7 (at t_a)
TOV	Hot	Δt_c	≈100	32.4(constant)	26.0(constant)
LCTT	Cold	end of cooling		39.8	28.1
LCTT	Hot	end of heating		33.4	32.8

TABLE VII
HIGHEST TOTAL FIELD DUE TO THE TOV OF FIG. 1 WITHIN Δt_a, Δt_b, Δt_c VS. HIGHEST DC FIELD AT LCTT VOLTAGE, WITH a_H, b_H

Voltage	Hot/cold cable	Time interval	Duration (ms)	Max.field at inner insul.(kV/mm)	Max.field at outer insul.(kV/mm)
TOV	Cold	Δt_a	≈5	39.3 (at t_a)	27.1 (at t_a)
TOV	Cold	Δt_b	≈5	39.3 (at t_a)	27.1 (at t_a)
TOV	Cold	Δt_c	≈100	34.5 (constant)	24.3 (constant)
TOV	Hot	Δt_a	≈5	34.2 (at t_a)	31.3 (at t_a)
TOV	Hot	Δt_b	≈5	34.2 (at t_a)	31.3 (at t_a)
TOV	Hot	Δt_c	≈100	29.5(constant)	28.6(constant)
LCTT	Cold	end of cooling		37.4	29.7
LCTT	Hot	end of heating		28.1	37.6

TABLE VIII
TOTAL LOSS-OF-LIFE FRACTIONS AT INNER INSULATION FOR THE TOV OF FIG.1 IN COLD AND HOT CABLE CONDITIONS WITH a_L, b_L, a_M, b_M AND a_H, b_H

	Cold Cable		Hot Cable	
Δt_c (ms)	100	200	100	200
loss-of-life fract.(a_L, b_L)	1.0×10^{-7}	1.9×10^{-7}	3.7×10^{-8}	7.0×10^{-8}
loss-of-life fract.(a_M, b_M)	2.6×10^{-8}	4.8×10^{-8}	6.0×10^{-9}	1.1×10^{-8}
loss-of-life fract.(a_H, b_H)	1.8×10^{-8}	3.3×10^{-8}	3.8×10^{-8}	7.0×10^{-9}

Table VIII proves that the life fraction lost during the TOV at inner insulation is higher for the Cold than for the Hot Cable, since the field is higher for the Cold than for the Hot Cable (see Figs. 8,10 vs. Figs. 9,11). The loss of life at inner insulation decreases as a,b increase, since the maximum field at inner insulation also decreases as a,b increase (compare Figs. 8,9 to Figs. 10,11 and Table VI to Table VII), thus inner insulation is progressively less stressed. Table VIII also shows that the life lost is particularly sensitive to the value of Δt_c, since the loss-of-life fraction increases by ≈85% as Δt_c is increased from 100 to 200 ms, thus an accurate estimation of such value is crucial.

IV. DISCUSSION

It can be argued that the field results reported in Section III should be regarded with care, since – as pointed out at Section II – they rely on the assumption that cable insulation is homogeneous, thus unaffected by local space charge

distributions at the electrodes and in the insulation bulk. Actually, in extruded polymeric insulation for HVDC cables local storage of space charge arises due to the inhomogeneities within the insulation, in particular: a) chemical traps, e.g. due to the presence of additives or of cross-linking by-products like acetophenone, alpha-metilstyrene, cumyl-alcohol; b) physical traps associated with imperfections of the macro-molecular structure of polymers, like kinks, bents, vacancies, etc.; c) nano-, meso-, micro- or macro-voids, or interfaces; d) metallic contaminants. Simulation of local charge distributions would require a very accurate knowledge of all such imperfections, which in turn would imply a precise knowledge of all features of the compounds – know exactly to each single manufacturer only. These simulations can be done – with huge computation complexities and under many simplifying hypotheses about the physical parameters implied – but they would depend strongly on the particular cases studied. Therefore the treatment would not have general validity and applicability, contrary to the aim of the methodology proposed here, i.e. having a simple and effective evaluation tool for a preliminary estimation of the field associated with TOVs, so as to enable also a general and overall comparison between different cable designs, different extruded materials (e.g. cross-linked vs. thermoplastic), etc.

The only alternative to simulation is direct measurement of space charge and subsequent computation of the space-charge "Poissonian" field, which obviously is even more strongly dependent on the particular cable measured.

On the other hand, R&D activities on HVDC extruded cable systems have shown that inhomogeneities associated with space charges have to be removed as much as possible to improve the space-charge behaviour and the electro-thermal performance of HVDC cables and accessories. Manufacturers have their own "recipes", especially as for dielectric compounding [13],[16]-[18], but overall making insulation as homogeneous as possible is the best practice to achieve well designed cables: those which – according to the state of the art technology of extruded cables, summarized in [12] – are able to pass qualification tests. Indeed, the voltage levels and duration of pre-qualification and type tests are determined in [12] by assuming the insulation as homogeneous: this is witnessed by the use of the IPM in the form of (13), with design and test voltage across whole insulation, irrespective of possible inhomogeneities within the insulation thickness. This notwithstanding in [12] space charge measurements "*left to the discretion of the manufacturer*" are recommended "*during the development testing*" prior to qualification tests of HVDC cable systems.

As a proof that well-designed HVDC cables can be treated as uniform and not particularly sensitive to space charge effects, it is observed in [18],[36] that well-designed and manufactured HVDC extruded cables according to the existing state-of-the-art – i.e. those passing the qualification tests prescribed in [12] – are expected to exhibit space charge effects on the local field that are <u>within</u> ≈10% of the design field of the cable, hence well covered by the typical safety coefficients used in cable design. Now these effects can be assessed directly at the qualification stage via space charge measurements done on full size cables following the prescriptions found in IEEE 1732-2017 [37].

For all these reasons, the proposed approach of calculating both electric field and loss-of-life under the hypothesis of homogeneous insulation appears as sound for well-designed cables, i.e. those that have been and are being currently manufactured, qualified after [12] and installed worldwide.

Coming to the fractions of life lost reported in Table VIII, they are in fact a sign that the long TOV causes a reduction of cable life, thus of cable reliability (see (14)). However, all life fractions lost in Table VIII are so low that their impact on cable life and reliability is negligible in practice. Indeed, according to [15] the typical failure rate of a submarine HVDC cable is ≈0.06 faults/year/100 km, involving 1 fault every ≈6 years in a 300 km-long line. Thus, based on [15] and Table VIII, the rate-of-occurrence of worst-case TOVs associated with faults in an HVDC line is so low that the relevant cumulated loss-of-life fraction over the service life of the cable line can be neglected.

V. Conclusions

The calculations reported here outline that the maximum field during the worst-case long TOVs encountered in VSC HVDC cable systems - occurring at the inner surface of cable insulation - is higher than the maximum field at inner insulation during Type-Test loading cycles after CIGRÉ TB 496 in both Cold Cable (= no load) and Hot Cable (= full load) conditions.

From computed electric fields, the values of total loss-of-life fraction at inner insulation have also been calculated, following an approach used only for cables under load cycling plus rated DC or AC voltage so far and applied here for the first time to a transient voltage superimposed onto rated DC voltage. The results in Table VIII suggest that the most challenging situation during the TOV occurs at the inner insulation of the Cold Cable with the lowest values of electrical conductivity coefficients of the dielectric. However, the loss of life computed for one single worst-case TOV is very small, thus it does not seem a major concern for the reliability of HVDC extruded cables, when considering the very low rate of occurrence of such long TOVs in VSC HVDC cable systems.

On the other hand, as shown from the literature in Part 2, it cannot be fully excluded that the field level and duration of the worst-case TOV might trigger fast charge packets in a few cable designs. Such fast charge packets might add to local space charges on which cable design relies and make the aging rate of cable insulation faster than that of the model used here for life loss estimation. If this were the case, the loss-of-life fraction estimates in Table VIII would not be enough conservative and tests other than Load Cycling Type Tests after TB 496 could assess quantitatively the potential threat of long TOVs.

In conclusion, from the electric field and loss-of-life estimations done in this paper - based on sound theories - as well as from existing literature, the consequences of temporary overvoltages on the reliability of HVDC VSC extruded cables seem quite limited. However, from an engineering viewpoint we do not think it is wise to disregard the issue altogether and stop investigations here. Indeed, VSC-HDVC cable systems are relatively new, thus a long-lasting service experience on these systems is lacking: in fact, further simulations of long TOVs (see work by CIGRÉ JWG B4/B1/C4.73) and dedicated tests

on cable insulation subjected to such TOVs are ongoing, but not completed yet. In addition, our preliminary study is focused on cables, but also the behavior of accessories (joints and terminations) in the presence of TOVs needs to be addressed, in order to have a complete picture of the overall effects of these TOVs on the full cable system - i.e. cable and accessories.

As for accessories, compared to cables they feature more complex geometry, different dielectrics, multiple interfaces, various field grading strategies, which require extensive and careful analyses that are beyond the scope of this paper. However, as the rated DC voltage of polymeric cables is increasing in new designs, this makes the DC field inversion within cable insulation more likely, which could add more criticality to the insulation screen interface in accessories in the presence of the long TOVs treated here. On the other hand, such TOVs are fast-varying voltage waveforms - superimposed onto and with the same polarity as the DC voltage – and their capacitive field affects inner more than outer insulation. Thus, it could be guessed that the treated TOVs should not be a major problem for the insulation screen interface in accessories. However, a dedicated analysis to accessories is needed before drawing such conclusion: it will be the subject of future studies.

In Part 2, superimposed switching impulses applied during Type Tests after TB 496 are analyzed similarly to the TOVs in order to check if superimposed impulses might be equivalent to long TOVs and could thus in principle replace dedicated tests.

VI. References

[1] Brochure CIGRÉ 86, *Overvoltages on HVDC cables*, CIGRÉ Joint Working Group 33/21/14.16, Aug. 1994.

[2] S. Mukherjee, M Saltzer, Y-J Häfner, and S Nyberg, "Cable overvoltage for MMC based VSC HVDC system: interaction with converters", Int. Colloquium on H.V. Insulated Cables, New Delhi, India, 2017.

[3] T. Karmokar, M. Saltzer, S. Nyberg, S. Mukherjee, and P. Lundberg, "Evaluation of 320 kV extruded DC cable system for temporary overvoltages by testing with very long impulse waveform," CIGRÉ Session 2018 paper B1-123, Paris, August, 2018, pp. 1-11.

[4] M. Saltzer et al., "Overvoltages experienced by DC cables within an HVDC transmission system in a rigid bipolar configuration", 10th Int. Conf. on Insul. Pow. Cables (Jicable'19), paper C5.1, Versailles (France), Jun. 23rd-27th 2019, pp. 1-6.

[5] F. B. Ajaei, and R. Iravani, "Cable surge arrester operation due to transient overvoltages under DC-side faults in the MMC HVDC link," *IEEE Trans. Power Del.,* vol. 31, no. 3, pp. 1213–1222, Jun. 2016.

[6] H. Saad, P. Rault, and S. Dennetière, "Study on transient overvoltages in converter station of MMC-HVDC links," *Electr. Power Syst. Res*, vol. 160, pp. 397–403, Jul. 2018.

[7] S. Dennetière, H. Saad, A. Naud, and P. Honda, "Transients on DC cables connected to VSC converters," 9th Jicable, paper A10.4, Versailles (France), 2015.

[8] M. Goertz, S. Wenig, S. Beckler, C. Hirsching, M. Suriyah, and T. Leibfried, "Analysis of Cable Overvoltages in Symmetrical Monopolar and Rigid Bipolar HVDC Configuration," *IEEE Trans. Power Deliv.,* vol. 35, no. 4, pp. 2097-2107, Dec. 2019.

[9] M. Goertz, S. Wenig, S. Beckler, C. Hirsching, M. Suriyah, and T. Leibfried, "Overvoltage characteristics in symmetrical monopolar HB MMC-HVDC configuration comprising long cable systems," Proc. Int. Conf. Power Syst. Transients, Perpignan, France , Jun. 2019, pp. 1-6.

[10] Brochure CIGRÉ, *Surge and extended overvoltage testing of HVDC Cable Systems*, CIGRÉ Joint Working Group B4/B1/C4.73, 2021.

[11] G. Mazzanti, P. Seri, B. Diban, and S. Stagni, "Preliminary experimental investigation of the effect of long temporary overvoltages on the reliability of HVDC extruded cables", 2020 IEEE International Conference on Solid Dielectrics (IEEE ICD 2020), Jul. 2020.

[12] Brochure CIGRÉ 496, Recommendations for testing dc extruded cable systems for power transmission at a rated voltage up to 500 kV, prepared by CIGRÉ Working Group B1-32, Apr. 2012.

[13] H. Ghorbani, M. Jeroense, C.-O. Olsson, and M. Saltzer, "HVDC cable systems—Highlighting extruded technology," *IEEE Trans. Power Del.*, vol. 29, no. 1, pp. 414–421, 2014.

[14] G. Mazzanti, and M. Marzinotto, Extruded Cables for High Voltage Direct Current Transmission: Advances in Research and Development, IEEE Press Series on Power Engineering, Wiley-IEEE Press, 2013.

[15] Brochure CIGRÉ 815, Update of Service Experience of HV Underground and Submarine Cable Systems, CIGRÉ Working Group B1.57, 2020.

[16] A. Bareggi, P. Boffi, S. Chinosi, S. Franchi Bononi, L. Guizzo, G. Lavecchia, M. Marzinotto, G. Mazzanti, and G. Pozzati, "Current and future applications of HPTE insulated cables systems," CIGRÉ Session 2018, Paper B1-307, pp. 1–8.

[17] M. Jeroense, P. Bergelin, T. Quist, A. Abbasi, H. Rapp, and L. Wang, "Fully qualified 640 kV underground extruded DC cable system," CIGRÉ Session 2018, paper B1-309.

[18] S.Nishikawa, K.Sasaki, K.Akita, M. Sakamaki, T. Kazama and K. Suzuki, "XLPE cable for DC link", SEI Techn. Rev., n. 84, pp.59 - 64, 2017.

[19] M.J.P. Jeroense, and P.H.F. Morshuis, "Electric fields in HVDC paper-insulated cables", *IEEE Trans. Dielectr. Electr. Insul.*, vol. 5, no. 2, pp. 225-236, Apr. 1998.

[20] R. N. Hampton, "Some of the considerations for materials operating under high-voltage, direct-current stresses," *IEEE Electr. Insul. Mag.,* vol. 24, no. 1, pp. 5–13, Jan./Feb. 2008.

[21] C.K. Eoll, "Theory of stress distribution in insulation of high voltage d.c. cables", Part I, *IEEE Trans. Electr. Insul.*, vol. EI-10, no. 1, pp. 27-35, Mar. 1975.

[22] Electric cables - Calculation of the current rating equations (100 % load factor) and calculations of losses, Standard IEC 60287, Part 1-1; 1-2, 1-3, 2-1, 3-1, Series, Ed. 3.0, 2020.

[23] Calculation of the Cyclic and Emergency Current Rating of Cables, Part 2: Cyclic Rating of Cables Greater Than 18/30 (36) kV and Emergency Ratings for Cables of All Voltages, Standard IEC 60853-2, Ed.1.0, 1989.

[24] G. Mazzanti, "Life estimation of HVDC cables under the time-varying electrothermal stress associated with load cycles", *IEEE Trans. Power Del.*, vol. 30, no. 2, pp. 931 – 939, Apr. 2015.

[25] G. Mazzanti, "Including the calculation of transient electric field in the life estimation of HVDC Cables subjected to load cycles", *IEEE Electr. Insul. Mag.*, vol. 34, no. 3, pp. 27-37, May/Jun. 2018.

[26] B. Diban, and G. Mazzanti, "The effect of temperature and stress coefficients of electrical conductivity on the life of HVDC extruded cable insulation subjected to type test conditions", *IEEE Trans. Dielectr. Electr. Insul.*, vol. 27, no. 4, pp. 1295-1302, Aug. 2020.

[27] M.A. Miner, "Cumulative damage in fatigue", *J. Appl. Mechanics*, Vol. 67, A163, Sep. 1945.

[28] G. Mazzanti, "Analysis of the combined effects of load cycling, thermal transients and electro-thermal stress on life expectancy of high-voltage ac cables", *IEEE Trans.Power Del.*, vol.22, no. 4, pp. 2000-2009, Oct. 2007.

[29] G. Mazzanti, "The combination of electro-thermal stress, load cycling and thermal transients and its effects on the life of high voltage ac cables", *IEEE Trans. Dielectr. Electr. Insul.*, vol. 16, no. 4, pp. 1168-1179, 2009.

[30] G.J. Anders, and M.A. El-Kady, "Transient ratings of buried power cables. Part 1: Historical perspective and mathematical model," *IEEE Trans. Power Del.*, vol. 7, no. 4, pp. 1724–1734, Oct. 1992.

[31] E. Chiodo, and G. Mazzanti, "Theoretical and practical aids for the proper selection of reliability models for power system components," *Int. Jou. Rel. and Safety*, vol. 2, no. 1/2, pp. 99-128, 2008.

[32] M. Cacciari, G. Mazzanti, and G.C. Montanari, "Comparison of maximum likelihood unbiasing methods for the estimation of the weibull parameters," *IEEE Trans. Dielectr. Electr. Insul.,* vol. 3, n. 1, pp. 18-27, Feb. 1996.

[33] G. Mazzanti, and M. Marzinotto, "More insight into the extension of pre-qualification test for HV and EHV AC extruded cable systems," IEEE CEIDP, Shenzen, China, Oct. 2013, pp. 917-920.

[34] P. Labra Francos, S. Sanz Verdugo, and S. Guyomarch, "New French-Spanish VSC link," CIGRÉ Session 2012, paper B4-110, pp. 1–15, 2012.

[35] http://b4.cigre.org/Publications/Other-Documents/Compendium-of-all-HVDC-projects/

[36] E. Ildstad, J. Sletbak, B.R. Nyberg, and J.E. Lan, "Factors affecting the choice of insulation system for extruded HVDC power cables", CIGRÉ Session 2004, paper D1-203.

[37] Recommended Practice for Space Charge Measurements in HVDC Extruded Cables for Rated Voltages up to 550 kV, IEEE 1732, 2017.